American Journal of Electromagnetics and Applications
2016; 4(2): 26-33
http://www.sciencepublishinggroup.com/j/ajea
doi: 10.11648/j.ajea.20160402.13
ISSN: 2376-5968 (Print); ISSN: 2376-5984 (Online)

Design of Magnetic Metamaterial with Cells of Dual-Layer Square Spiral Resonators

Liqun Hua, Binyang He, Xianghong Kong, Gaobiao Xiao

Key Laboratory of Ministry of Education of Design and Electromagnetic Compatibility of High Speed Electronic System, Shanghai Jiao Tong University, Shanghai, China

Email address:
johnnylili@sjtu.edu.cn (Liqun Hua), gaobiaoxiao@sjtu.edu.cn (Gaobiao Xiao)

To cite this article:
Liqun Hua, Binyang He, Xianghong Kong, Gaobiao Xiao. Design of Magnetic Metamaterial with Cells of Dual-Layer Square Spiral Resonators. *American Journal of Electromagnetics and Applications.* Vol. 4, No. 2, 2016, pp. 26-33. doi: 10.11648/j.ajea.20160402.13

Received: November 14, 2016; **Accepted**: November 28, 2016; **Published**: January 6, 2017

Abstract: Artificially constructed materials, including metamaterials with negative magnetic permeability (μ) at megahertz frequencies, have been applied in various fields and the construction of new devices. Among these applications, the split-ring resonators (SRRs) and spiral resonators (SRs) are the most widely used metamaterial cells, especially in telemetry and antenna systems proposed in the past few years. In this paper, one particular cell, whose structure is square spiral wires printed on both sides of a dielectric substrate, is selected as the investigated resonator. Numerous simulations are conducted to study the properties of both magnetic resonance and effective permeability. The effect of the geometrical parameters on the resonance frequency and the impact of the number of turns of spiral resonator on the permeability are investigated. The effective permeability of the periodic SR array varies with the metal width and the gap spacing. The values of μ are extracted at a chosen frequency of 29.8 MHz, based on which the geometrical parameters of the SR array whose relative permeability is -1 can be determined. This kind of artificial magnetic materials are able to be used for improving the efficiency of a wireless power transfer system.

Keywords: Metamaterial, Spiral Resonator (SR), Negative Permeability, Wireless Power Transfer (WPT)

1. Introduction

Metamaterials have stepped into the practical application period from aforetime designing and experimental stage. The concept of metamaterial and its structure were first proposed by J. B. Pendry et al. [1]. Since then, materials with artificial structure aligned in periodic arrays have attracted intense research mainly in millimeter wave and terahertz frequency band. Recently, metamaterials used at low radio frequencies have received considerable attentions and many articles concentrate on the design and analysis of them [2]-[4]. These metamaterials employed under 100 MHz also have a wide variety of usage scenarios, such as near field imaging [5]-[6], enhancement of charging portable battery-powered electronics and electric vehicles [7], highly-directional energy transfer antenna [8]-[9] and so on.

In the past, planar spirals are recognized structures in microwave engineering, where they are generally presented as lumped inductors [10]. However, a few artificial metamaterials have been designed by using spirals as the unit cells in recent years [11]. A low-MHz resonant frequency of metamaterial is the primary condition for designing metamaterial used in low frequency case, which has certain requirements on their structure and geometrical parameters. It is validated in [12] that an SR achieves a lower resonant frequency than an SRR for the same dimension of cell. In addition, square SR has the advantages of making full use of substrate area and easy fabrication process, therefore, square spiral resonator is often introduced in metamaterial designs [13]-[15]. Similarly, we can attain a resonance occurring at lower frequency than single-sided designs by adding another spiral layer, in which the capacitance is drastically increased by broadside metallic surfaces with large area and its small interlayer dielectric spacing. Meanwhile, larger effective inductance is obtained as well using multi-turns of spirals. Many literatures present the duplex printed resonant as the cell for metamaterials [16]-[18].

When it comes to metamaterials, artificial electromagnetic materials with both negative permittivity and negative permeability, which are known as left-handed materials

(LHM), are referred in most literatures. LHMs have the properties of negative refractive index and opposite directions between wave vector and Poynting vector, which are caused by negative ε and negative μ. So there will be a focusing phenomenon of the refracted wave for a plate with a certain thickness. Nevertheless, in low-frequency quasi-static limitation, metamaterials put in megahertz applications satisfy the near-field condition where magnetic and electric fields are almost decoupled. On this occasion, magnetic response of the metamaterial is dominant components to be considered, and only permeability is required to be negative. In other words, metamaterials with negative μ and positive ε can perform similarly to double negative metamaterials at low frequencies.

Effective medium approximation theory is necessary for the investigation of the magnetic properties of metamaterials. In order to use the homogenization method appropriately and accurately, wavelengths need to be much larger than the size of unit cell [19]-[21]. In [21], the reported individual cell, which is called extremely sub-wavelength metamaterial, has a great effective medium ratio (λ/a) of 744, that is, the scale of the resonant wavelength to its length. Although the surge on the design of magnetic metamaterial at low operating frequencies has been fueled during these years, explorations of tuning its resonant frequencies have been relatively rarely reported. In this paper, we take a simulation method in showing that the resonance frequency of the dual-layer square spiral resonator varies with its geometrical parameters like metal width, gap spacing and surface size. After that, *S*-parameter retrieval approach proposed by D. R. Smith et al. [22] is adopted to calculate the effective μ and ε from reflection and transmission coefficients of this magnetic metamaterial to find the frequency region in which condition of $\mu(\omega) < 0$ is met. Then, the resonator with certain parameters is chosen as the unit cell of a 4×4 planar array, which is applied in wireless power transfer system. The efficiency of the system can be promoted by 17% through placing the metamaterial slab at the halfway position of the transmitter and the receiver.

Besides traditional SR and SRR structure, there are various metamaterials derived from those old-style structures [23]-[25]. Our investigation also holds true for the adjustment of modified version magnetic resonators. The remainder of this paper is arranged as follows. In section II, the dependence of resonance frequency on certain geometrical parameters is studied. The impact of spiral resonator's number of turns on the permeability is reported in section III and the results of permeability of the spiral resonator with different metal widths and lengths of gaps at 29.8 MHz are discussed. One of the applications of dual-layer square SR is demonstrated in section IV. Conclusions are presented in section V.

2. Effect of Geometrical Parameters on the Resonance Frequency

The resonators under investigation have nearly the same structure and parameters reported in [26], except that there is no metallic via between the two layers. They are made by two single strips tucked up to form two square spirals respectively and printed on two sides of a dielectric substrate, as shown in figure 1. The cells with size a = 65 mm are fabricated on circuit boards with dielectric value of 3.55 and thickness of 1.5 mm. The square spirals on each side are metallic traces with bulk conductivity of $\sigma = 5.8 \times 10^7$ S/m, strip width of w = 3 mm, gap spacing of t = 1 mm between neighboring traces and copper thickness of 70 μm. The width of copper structure is 61 mm.

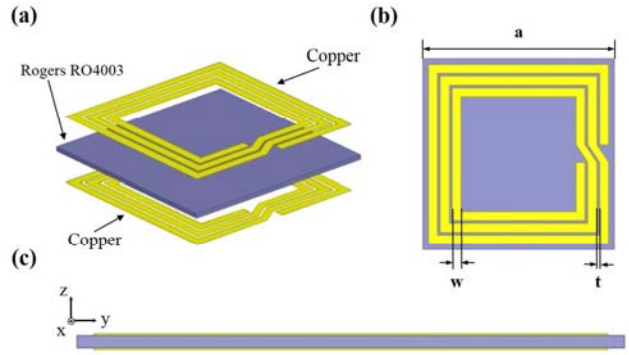

Figure 1. *Schematic drawings of the dual-layer square spiral metamaterial unit cell. (a) In the exploded view. (b) In the top view. (c) In the side view.*

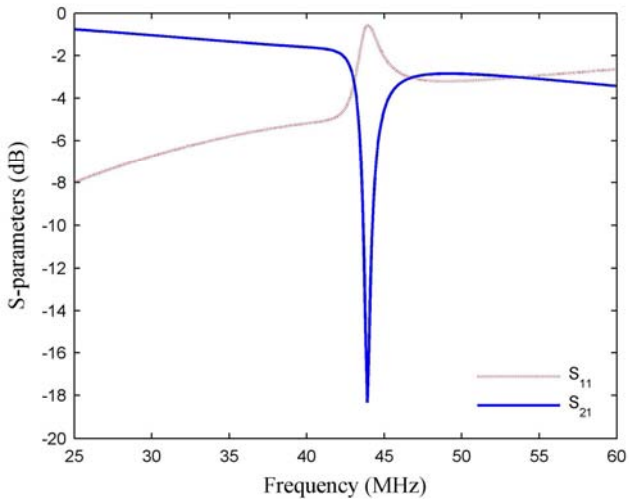

Figure 2. *Simulated reflection coefficient (S_{11}) and transmission coefficient (S_{21}) of individual double-sided square spiral resonator unit.*

Simulations are done with a commercial finite-element tool, which is ANSYS HFSS. The metamaterial unit cell is subjected to an incident plane wave propagating along the *y*-direction, as shown in figure 1(c). In HFSS, periodic boundary conditions are set where magnetic field is along negative *z*-axis and electric field is along *x*-axis. The considered structure is assumed to be infinitely periodic along two directions that are perpendicular to the direction of propagation. We can see a cutoff band and a dip in the curve of transmission coefficient in figure 2. The frequency where the dip is located at is the resonant frequency of the studied structure, which is found to be 43.9 MHz.

The cutoff band and the dip observed in the S_{21} curve can be

attributed to strong magnetic response of incident wave. Magnetic resonance is mainly induced by two contributions, one from capacitance arising by nearby gaps between metal strips and mutual interaction of bilayer wires, the other from inductance of all metallic traces in SR. This section covers the change of resonant frequency with the metal width (w), gap spacing (t) and surface size (a). The effect of these parameters will be introduced in detail below.

A. Changing Metal Width

As is well-known, the resonant frequency is given by

$$\omega_0^2 = 1/LC\,, \tag{1}$$

where C is the capacitance of the suitable equivalent resonant circuit and L may be estimated using formulae in [10]. We study the effect of metal width on ω_0 of the individual double-sided spiral resonator by remaining other parameters constant and only changing its metal width. The initial parameters are taken to be w = 3 mm, t = 1 mm and a = 65 mm as plotted in figure 1(b). Simulations are performed on 20 samples with metal width varied from 0.3 mm to 6 mm with steps of 0.3 mm.

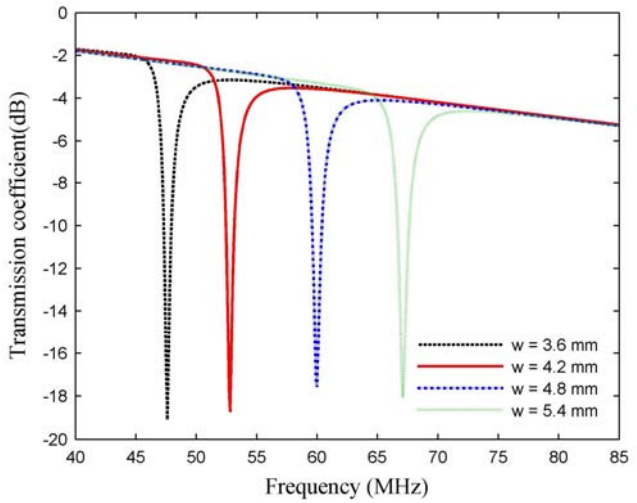

(a)

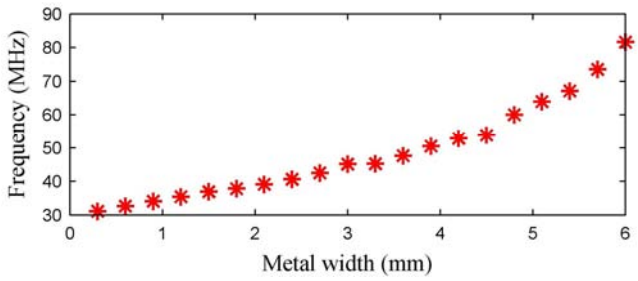

(b)

Figure 3. *(a) Transmission coefficients of four different metal widths determined from simulations of single unit of SR. (b) Sketch of resonant frequencies varying with twenty metal widths.*

The simulated magnitude of the transmission coefficient of individual SR with four different metal widths is provided in figure 3(a). Resonant behavior is observed for all structures and magnetic resonant frequency gets higher with increasing metal width. The same phenomenon can be seen in figure 3(b) that resonant frequency shows as a function of metal width and ω_0 is monotonically increasing with respect to w. It can be interpreted that metal width affects all inductances and capacitances of SR. The augment of metal width results in the decrease of mutual inductance and capacitance. Therefore, if we have to design a metamaterial used in higher frequency range, we can increase metal width of every SRs. For the same reason, SRs made of thinner metal width have lower resonant frequency.

B. Changing Gap Spacing

We change all gap spacings between every metallic traces of single unit of SR while the other parameters are left unchanged (w = 3 mm, a = 1 mm). When we fix the metal width, an increase of gap spacing is equivalent to reducing effective capacitance. Figure 4(a) shows magnitude of the transmission coefficient of individual SR with gap spacings obtained via simulation. Furthermore, notice that both drawings of S_{21} curves in figure 3(a) and figure 4(a) are in the presence of same steps of 0.6 mm. It can be seen from figure 3 and figure 4 that greater modification of resonant frequency can be achieved by changing gap spacing instead of altering metal width.

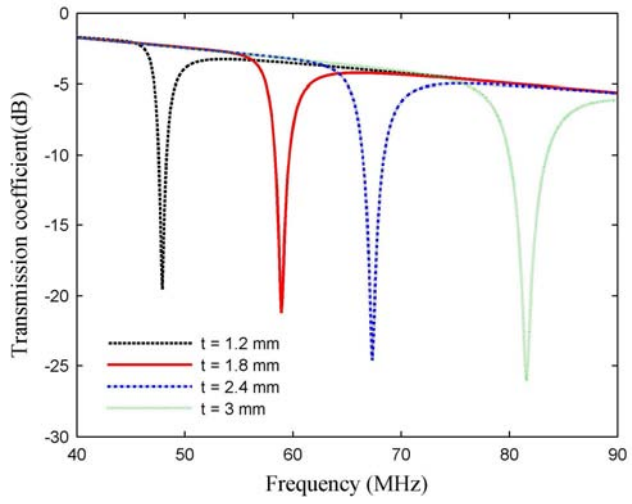

(a)

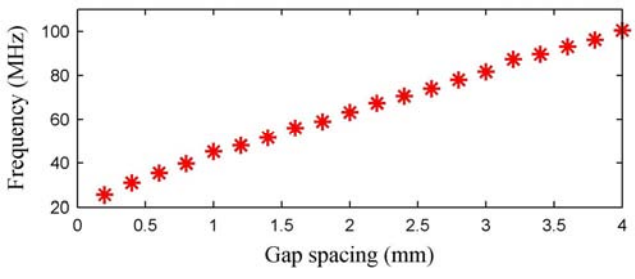

(b)

Figure 4. *(a) Transmission coefficients of four different gap spacings determined from simulations of single unit of SR. (b) Sketch of resonant frequencies varying with twenty gap spacings.*

Variation of magnetic resonant frequency of metamaterial cell with different gap spacings from 0.2 mm to 4 mm with

steps of 0.2 mm is provided in figure 4(b). Results of simulations display that ω_0 of the individual SR increases with gap spacing between neighboring wires. The situation is similar to previously reported analytical model [27] of split-ring resonator which gives an explanation that enlarging gap spacing reduces both mutual capacitance and inductance of equivalent LC circuit of SRR. The shrunk of capacitance and inductance consequently lead to a higher resonant frequency according to equation (1).

C. Changing Surface Size

Next, we exhibit the influence of surface size on the targeted cell resonant frequency. The other two parameters are kept constant (w = 3 mm, t = 1 mm) and we only vary the length of cell with 5 mm steps between 45 and 90 mm. The frequency where resonance happens and surface size are inversely proportional, as shown in figure 5. When a bigger metamaterial unit cell by scaling up the original design mentioned at the beginning of this section is manufactured, the mutual inductance and capacitance correspondingly become larger, which brings about the rapid decline of ω_0. Along with the descending of resonant frequencies, the ohmic losses in metamaterial slab become greater. Accordingly, there is a compromise between low-frequency operation and low-loss square spiral resonator. In general, metamaterials with low-MHz resonance won't be produced by the construction of large dimension cell due to the poor performance of the metamaterial in practical applications. As a consequence, we often define a fixed surface size of the spiral resonator and change metal widths and gap spacings when resonant frequency point needs to be adjusted.

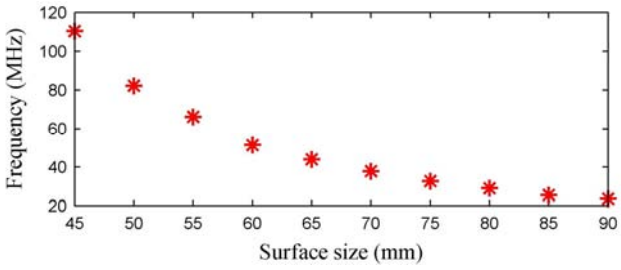

Figure 5. *Sketch of resonant frequencies varying with ten surface sizes.*

3. Impact of Metamaterial Structure on the Effective Permeability

Up to this point, we just regulate the geometrical parameters of individual SR in place of changing the whole structure. It is quite clear that the resonant frequency will drift if the turns of metallic traces are changed. However, in terms of the original parameters (a = 65 mm, w = 3 mm, t = 1 mm) taken in section II, the number of turns is at most seven. Thus, we adjust the original parameters to make more turns available on the dielectric board. The new unit of dual-layer square spiral resonator with metal width of 1 mm, gap spacing of 0.6 mm, wires of 4 turns and unaltered surface size of 65 mm is adopted.

Numerical simulation displays that the resonant frequency of the metamaterial unit cell with the new structure is at 24.9 MHz. Applying the retrieval method proposed in [22], we can calculate the effective permeability of the metamaterial unit cell. As plotted in figure 6, the real part of permeability extracted from simulated S-parameters has both positive and negative values in different frequency region. What's more, the single cell always has a negative permeability above the resonant frequency. In the meantime, there exists a few discontinuous points of the imaginary part of permeability near the resonance of 24.9 MHz. It is caused by the deficiency of the retrieve method when the real part of impedance is close to zero [28].

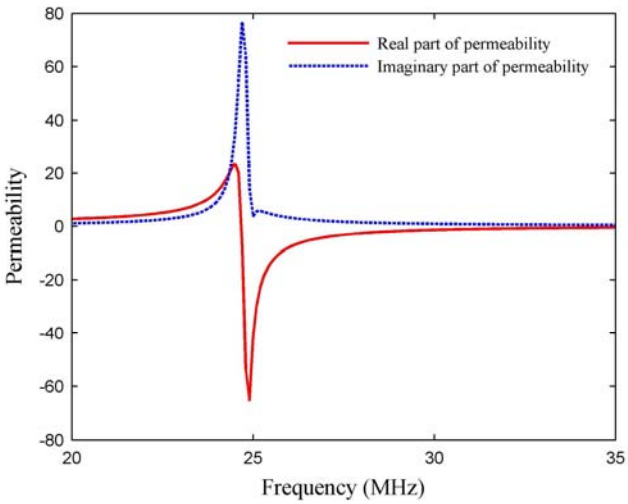

Figure 6. *Extracted magnetic permeability of the cell with four turns by employing the retrieval procedure.*

The effective permeability points with small errors don't influence our study of applying them to wireless power transfer systems, since the permeability values of around -1 are taken into consideration in these situations. The reason why permeability is chosen to be -1 and the advantages are described in [29], where an isotropic perfect lens with ε = -1 and μ = -1 is introduced. As introduced in section I, the metamaterial in the range of the low frequencies may be seen as quasi-magnetostatic state, the effect of permittivity is not necessary to consider. Consequently, units of dual-layer square SRs with μ = -1 are enough in various megahertz applications. In the structure of four-turn wires, a permeability of -1 is obtained at 31.3 MHz where the losses are also kept tiny.

Variation of resonant frequency and -1 permeability frequency of double-sided square spiral resonator with different numbers of turns from two to ten is provided in figure 7. In all cases, the permeability of -1 in the frequency band invariably emerges after resonant frequency. The diminution of frequency point where resonance and μ = -1 occur with increasing the number of turns is observed. The frequency possessing permeability value of -1 is of special usage and is obtained with simulation for the new structure. It is shown in figure 8 as a function of $f(w,t)$. This frequency will drop by decreasing metal width or reducing gap spacing, which is similar to the effects of metal width and gap

spacing on resonant frequency. The minimum frequency is taken at (w,t) = (0.2,0.2), which is 19.6 MHz and the maximum frequency is taken at (w,t) = (2,2), which is 58.5 MHz. It can help us to locate μ = -1 frequency at the desired operation by adjusting the two size parameters of the investigated structure in designing metamaterial.

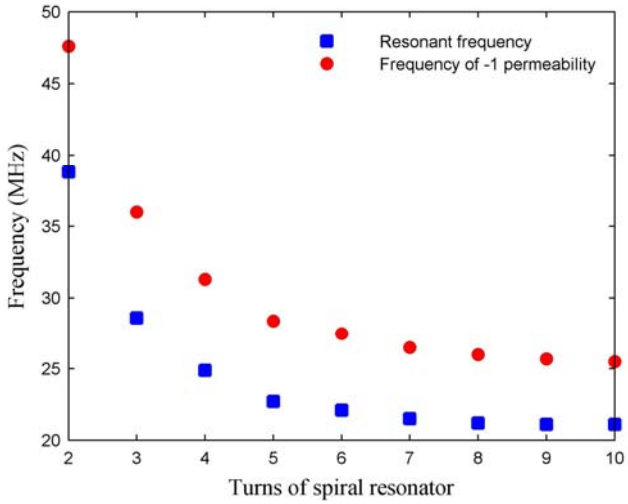

Figure 7. *Exhibition of the resonant frequency and the frequency where permeability has the value of -1 versus number of turns.*

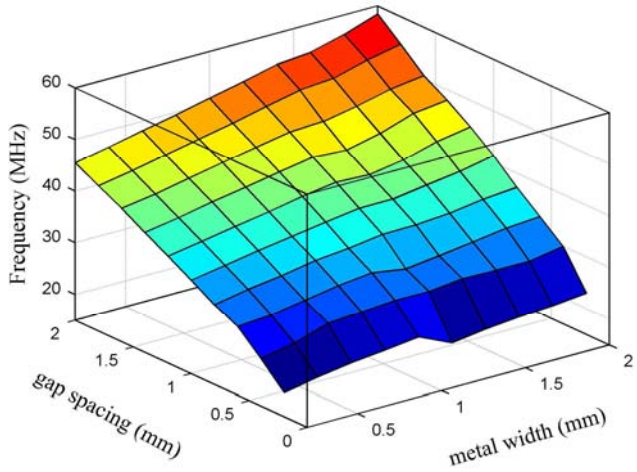

Figure 8. *The frequency where permeability value μ = -1 varying as a function of metal width and gap spacing.*

Sometimes, the permeability of metamaterial has to be modified at a fixed frequency. Therefore, we make several simulations at a selected frequency, which is 29.8 MHz here, to explore the respective relationship between the permeability and metal width, gap spacing. Color diagrams and contour maps are used to demonstrate $\mu(w,t)$, as plotted in figure 9. The contours are able to give a good reference to find the appropriate combination of w and t at 29.8 MHz when an expected permeability has to be taken. Figure 9 also displays that the permeability of single unit of SR with big w and t is a little greater than zero and the permeability of individual SR with small w and t is appreciably less than zero at 29.8 MHz.

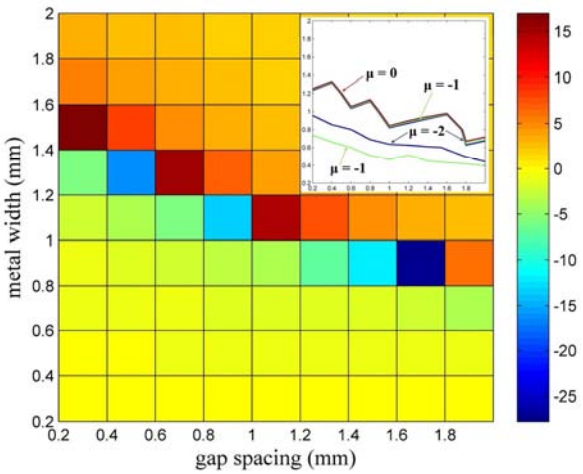

Figure 9. *Color diagrams and contour maps of permeability as a function of the critical parameters w and t of the new double-sided spiral resonator cell at 29.8 MHz.*

It has been known that -1 permeability can be taken at (w,t) = (0.6,0.6) in the contour map when frequency is 29.8 MHz. The point is included in the red dotted curve of t = 0.6 mm whose μ is on the decline gradually from -0.72 to -5.64 with the increase of w, as shown in figure 10(a). In the black curve of t = 0.2 mm, the permeability changes little and is almost a negative horizontal line very close to zero. It can be interpreted as the resonance happens far below 29.8 MHz regardless of the value of w when t is 0.6 mm. The permeability is always above zero whatever the value of w is in the green curve of t = 1.4 mm, which is for the reason that the resonant frequency is above 29.8 MHz as t is 1.4 mm. Pay attention that the resonant frequency is hard upon 29.8 MHz as w is 0.2 mm, which lead to a permeability of positive and high value. In the blue curve of t = 1 mm, the permeability experiences a process from negative to positive in the range from -13.53 to 14.83.

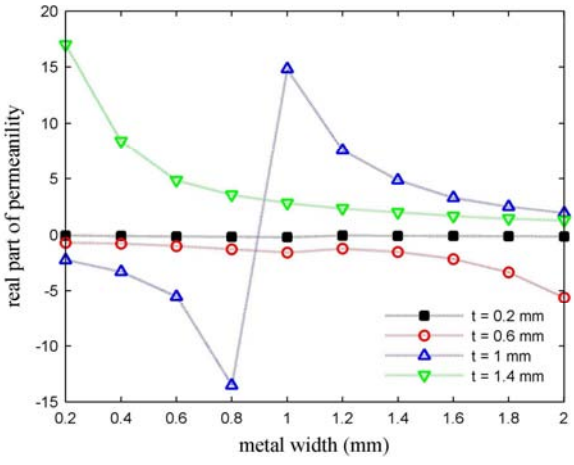

(a)

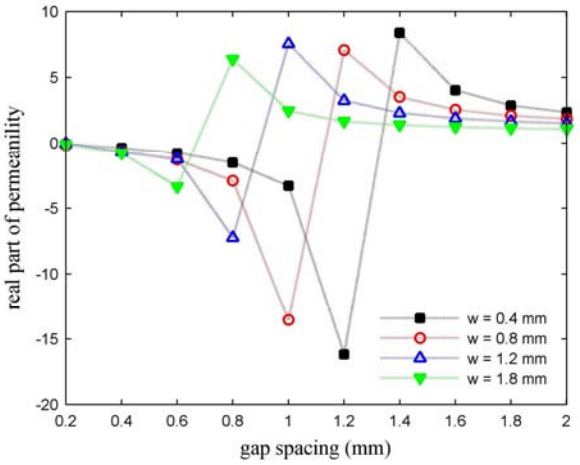

(b)

Figure 10. *Real part of the effective permeability at 29.8 MHz. (a) Varying with metal width. (b) Varying with gap spacing.*

The study on the permeability and gap spacing of one-to-one correspondence with a determined *w* is illustrated in figure 10(b), as a complement to figure 9. The magnetic permeability of four curves all go through from low negative values to high positive values, which stands for resonance's undergoing from below 29.8 MHz to above 29.8 MHz. In addition, no matter what *w* is taken from 0.2 mm to 2 mm in the simulations, -1 permeability is always available by altering the value of *t* in a relatively small scope. For comparison, there is no such observation in figure 10(a), which signifies that gap spacing has a higher sensitivity to permeability and resonant frequency than metal width of double-sided square spiral resonator.

4. Spiral Resonators Array in Wireless Power Transfer

A regular array of dual-layer square spiral resonators is applied in the wireless power transfer system at a resonance frequency of 29.3 MHz, which is one of various applications of magnetic metamaterial. When the metamaterial slab is inserted between the transmitting coils and receiving coils, the power transfer efficiency of the system is promoted by the confinement of magnetic fields between the coils, as illustrated in figure 11.

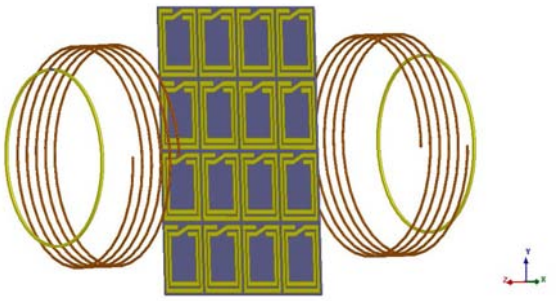

Figure 11. *Schematic drawing of wireless power transfer system showing the transmitter, the receiver and the metamaterial slab with cell of dual-layer square spiral resonators.*

In this system, the receiving coils made up of a primary coil with a diameter of 8 cm and a secondary coil with a diameter of 20 cm are exactly same with the transmitting coils. The primary coil is added in series with a capacitance of 20 pF, which is inductively coupled to the two-centimeter-distance secondary coil. The secondary coil is in the presence of a five-turn helix with neighboring pitch of 1 cm and copper radius of 1 mm, which is resonantly coupled to another twenty-six-centimeter- distance secondary coil of receiver.

The metamaterial slab consists of 4 × 4 unit cells with the size of 260 mm × 260 mm. The units of SRs with the parameters presented in section III have the real value of permeability of -1.13 at 29.3 MHz. In this case, the evanescent wave is amplified on the two surfaces of the metamaterial slab. As shown in figure 12, the magnetic field distributions of WPT systems with magnetic metamaterial composed of dual-layer square spiral resonators and without a metamaterial slab are compared. The strength of magnetic field shows that the magnetic induction lines are re-converged as they pass the metamaterial slab. Thus the power in case (b) which has the highest magnetic flux density shows a significant improvement compared to case (a).

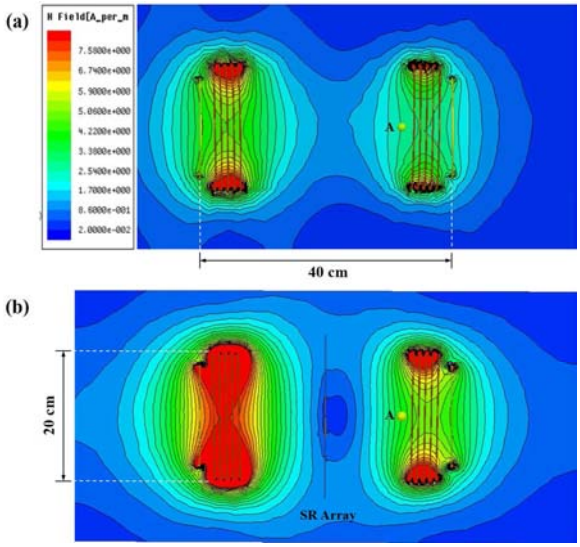

Figure 12. *The simulated magnetic field distribution in the WPT system with four coils. (a) Without metamaterial. (b) With a magnetic metamaterial slab.*

The point A in figure 12 is used to make a quantitative comparison between case (a) and case (b) of the magnetic field strengths among the transmitting and receiving coils. The intensity of magnetic flux at point A increases from 65.8 mG to 73 mG when the spiral resonators array is positioned toward the halfway plane between the transmitter and the receiver, as reported in Table I. Since the WPT system operating through near-field resonant coupling can be modeled as a two-port network. The power transfer efficiency can be defined as [19]

$$\eta = \frac{|S_{21}|^2}{1-|S_{11}|^2} \tag{2}$$

Table 1. *Simulated results of efficiency with and without metamaterial slab at 40 cm distance.*

At 40 cm distance	With An Array of SRs	Without Metamaterial
S_{21} (ω_0)	-5.72	-4.08
Magnetic flux density (point A)	65.8mG	73mG
Maximum value of efficiency	31.9%	48.9%

The results of the maximum value of efficiency at the primary-coil-to-primary-coil distance of 40 cm are also listed in Table I.

As the distance between the transmitters and the receivers is 40 cm, the efficiencies of WPT systems with different configurations obtained from simulations are plotted in figure 13. The curve (a) represents the efficiency as a function of frequency when there are no metamaterials in the system. A peak exists near the resonant frequency of the transmitting coils and the peak efficiency about 31.9% is achieved. After putting the metamaterial slab of spiral resonators array in the middle of the system, power transfer efficiency improves and the peak efficiency is observed to be about 48.9%. The position of maximum value of efficiency is shifted by reason of the modified mutual coupling among the transmitting coils, the metamaterial with units of dual-layer square spiral resonators, and the receiving coils.

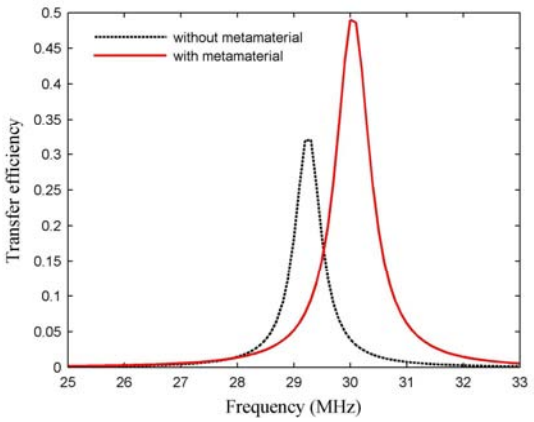

Figure 13. *The power transfer efficiency of two system configurations: the initial system without metamaterial and the improved WPT system with periodic arrays of SRs.*

Therefore, the proposed structure is an effective design to focus the magnetic fields and gain a higher efficiency by arranging a number of unit cells to form a metamaterial slab with the negative permeability in the WPT system. On the other hand, the enhancement of the power transfer efficiency implies that the alteration in the opposite direction of magnetic fields caused by -1 permeability overcomes the bad effect of array's losses. The result of the work shows that the design of megahertz metamaterials with negative permeability is of great applicable significance to the wireless power transfer.

5. Conclusions

The influence of metal width, gap spacing, surface size and number of copper turns on the resonance frequency of an individual SR are explored. Increasing the metal width and gap spacing gives rise to higher resonance frequencies. Enlarging the surface size causes the deterioration of resonance frequency. Increasing the number of copper turns leads magnetic resonance to a lower frequency. The desired frequency and permeability is available by adjusting metal width and gap spacing appropriately. Furthermore, it is found that in SRs a greater modification of resonance frequency and permeability can be obtained by changing gap spacing instead of altering metal width. The efficiency of the WPT system is enhanced by 17% as this kind of metamaterials with cells of dual-layer square spiral resonators are proposed to be used.

References

[1] J. B. Pendry, A. J. Holden, D. J. Robbins, and W. J. Stewart, "Magnetism from conductors and enhanced nonlinear phenomena," *IEEE Trans. Microw. Theory Techn.*, vol. 47, no. 11, pp. 2075-2084, Nov. 1999.

[2] C. Kurter, J. Abrahams, and S. M. Anlage, "Miniaturized superconducting metamaterials for radio frequencies," *Appl. Phys. Lett.*, vol. 96, no. 25, pp. 3504 1-3, Jun. 2010.

[3] F. Bilotti, and L. Sevgi, "Metamaterials: Definitions, properties, applications and FDTD-based modeling and simulation," *Int. J. RF and Microw. Computer-Aided Eng.*, vol. 22, no. 4, pp. 422-438, Apr. 2012.

[4] E. S. G. Rodriguez, A. K. RamRakhyani, D. Schurig, and G. Lazzi, "Compact low-frequency metamaterial design for wireless power transfer efficiency enhancement," *IEEE Trans. Microw. Theory Techn.*, vol. 64, no. 5, pp. 1644-1654, May 2016.

[5] M. C. K. Wiltshire, "Radio frequency (RF) metamaterials," *Phys. Status Solidi B*, vol. 224, no. 4, pp. 1227-1236, Apr. 2007.

[6] M. A. Lopez, M. J. Freire, J. M. Algarin, et al., "Nonlinear split-ring metamaterial slabs for magnetic resonance imaging," *Appl. Phys. Lett.*, vol. 98, no. 13, pp. 3508 1-3, Mar. 2011.

[7] W. X. Zhong, X. Liu, and S. Y. R. Hui, "A novel single-layer winding array and receiver coil structure for contactless battery charging systems with free-positioning and localized charging features," *IEEE Trans. Ind. Electron.*, vol. 58, no. 9, pp. 4136-4144, Dec. 2011.

[8] M. M. Falavarjani, M. Shahabadi, and J. Rashed-Mohassel, "Design and implementation of compact WPT system using printed spiral resonators," *Electronics Lett.*, vol. 50, no. 2, pp. 110-111, Jan. 2014.

[9] C. Y. Liou, C. J. Kuo, S. S. Lin, and S. G. Mao, "Printed spiral metamaterial resonators for wireless powering system with proximal metal plates," *IEEE Int. Symp. Radio-Frequency Integration Technology (RFIT),* pp. 70-72, Aug. 2015.

[10] Z. M. Hejazi, P. S. Excell, and Z. Jiang, "Accurate distributed inductance of spiral resonators," *IEEE Microw. guided wave lett.*, vol. 8, no. 4, pp. 164-166, Apr. 1998.

[11] O. Isik, and K P. Esselle, "Analysis of spiral metamaterials by use of group theory," *Metamaterials*, vol. 3, no. 1, pp. 33-43, Mar. 2009.

[12] J. D. Baena, R. Marques, F. Medina, and J. Martel, "Artificial magnetic metamaterial design by using spiral resonators," *Phys. Rev. B*, vol. 69, no. 1, pp. 4402 1-5, Jan. 2004.

[13] P. Gay-Balmaz, and O. J. F. Martin, "Electromagnetic resonances in individual and coupled split-ring resonators," *J. Appl. Phys.*, vol.92, no. 5, pp. 2929-2936, Aug. 2002.

[14] F. Bilotti, A. Toscano, and L. Vegni, "Design of spiral and multiple split-ring resonators for the realization of miniaturized metamaterial samples," *IEEE Trans. Antennas Propag.*, vol. 55, no. 8, pp. 2258-2267, Aug. 2007.

[15] Q. Wu, Y. H. Li, N. Gao, et al., "Wireless power transfer based on magnetic metamaterials consisting of assembled ultra-subwavelength meta-atoms," *Europhysics Lett.*, vol. 109, no. 6, pp. 68005 1-6, Mar. 2015.

[16] W. C. Chen, C. M. Bingham, K. M. Mak, et al., "Extremely subwavelength planar magnetic metamaterials," *Phys. Rev. B*, vol. 85, no.20, pp. 1104 1-5, May 2012.

[17] B. Wang, W. Yerazunis, and K. H. Teo, "Wireless power transfer: Metamaterials and array of coupled resonators," *Proc. IEEE*, vol. 101, no. 6, pp. 1359–1368, Jun. 2013.

[18] G. Lipworth, J. Ensworth, K. Seetharam, et al., "Magnetic metamaterial superlens for increased range wireless power," *Scientific reports*, vol. 4, pp. 3642 1-6, Jan. 2014.

[19] Y. Fan, and L. Li, "Efficient wireless power transfer by using highly sub-wavelength negative index metmaterials," *IEEE Int. Wireless Symp. (IWS)*, pp. 1–4, Apr. 2013.

[20] S. Zhong, and S. He, "Ultrathin and lightweight microwave absorbers made of mu-near-zero metamaterials," *Scientific reports*, vol. 3, pp. 2083 1-5, Jun. 2013.

[21] A. Rajagopalan, A. K. RamRakhyani, D. schurig, and G. Lazzi, "Improving power transfer efficiency of a short-range telemetry system using compact metamaterials," *IEEE Trans. Microw. Theory Techn.*, vol. 62, no. 4, pp. 947-955, Apr. 2014.

[22] D. R. Smith, S. Schultz, P. Markos, and C. M. Soukoulis, "Determination of effective permittivity and permeability of metamaterials from reflection and transmission coefficients," *Phys. Rev. B*, vol. 65, no. 19, pp. 5104 1-5, Apr. 2002.

[23] Z. Liang, T. Feng, S. Lok, et al., "Space-coiling metamaterials with double negativity and conical dispersion," *Scientific reports*, vol. 3, pp. 1614 1-6, Apr. 2013.

[24] Y. Zhang, H. Tang, C. Yao, et al., "Experiments on adjustable magnetic metamaterials applied in megahertz wireless power transmission," *AIP Advances,* vol. 5, no. 1, pp. 017142 1-9, Jan. 2015.

[25] Y. Cho, S. Lee, S. Jeong, et al., "Hybrid metamaterial with zero and negative permeability to enhance efficiency in wireless power transfer system," *IEEE Wireless Power Transfer Conf. (WPTC)*, pp. 1-3, May 2016.

[26] B. Wang, K. H. Teo, T. Nishino, et al., "Wireless power transfer with metamaterials," *IEEE Proc. 5th Eur. Conf. Antennas Propag. (EuCAP)*, pp. 3905-3908, Apr. 2011.

[27] R. Sauviac, C. R. Simovski, and A. Tretyakov, "Double split-ring resonators: Analytical modeling and numerical simulations," *Electromagnetics*, vol. 24, no. 5, pp. 317-338, Jun. 2004.

[28] X. Chen, T. M. Grzegorczyk, B.-I. Wu, et al., "Robust method to retrieve the constitutive effective parameters of metamaterials," *Phys. Rev. E*, vol. 70, no. 1, pp. 6608 1-7, Jul. 2004.

[29] J. B. Pendry, "Negative refraction makes a perfect lens," *Phys. Rev. Lett.*, vol. 85, no. 18, pp. 3966–3969, Oct. 2000.